IEEE Access
Multidisciplinary | Rapid Review | Open Access Journal

Received 10 June 2023, accepted 16 July 2023, date of publication 24 July 2023, date of current version 1 August 2023.

Digital Object Identifier 10.1109/ACCESS.2023.3298547

RESEARCH ARTICLE

Hardware in the Loop Real-Time Simulation of Improving Hosting Capacity in Photovoltaic Systems Distribution Grid With Passive Filtering Using OPAL-RT

MOHAMED A. ISMEIL[1,2], (Member, IEEE), AHMED ALFOULY[2], HANY S. HUSSEIN[1,3], (Senior Member, IEEE), AND I. HAMDAN[2]

[1]Electrical Engineering Department, Faculty of Engineering, King Khalid University, Abha 61411, Saudi Arabia
[2]Electrical Engineering Department, Faculty of Engineering, South Valley University, Qena 83523, Egypt
[3]Electrical Engineering Department, Faculty of Engineering, Aswan University, Aswan 81528, Egypt

Corresponding author: I. Hamdan (Ibrahimhamdan86@eng.svu.edu.eg)

This work was supported by the Deanship of Scientific Research at King Khalid University through Large Group Research Project under Grant RGP.2/162/44.

ABSTRACT The industrial revolution in the world resulted in a rise in the desire for energy in recent years. Therefore, the trend was strong toward the utilization of alternative and sustainable energy sources, such as solar power and wind energy. However, the growing prevalence of Distributed Energy Resources (DER) systems in the electricity network, cause several issues and operational restriction violations, including high and low voltage levels exaggerative transmission power dissipation, excess power consumption of distribution transformers and supply lines, protection breakdown, and high harmonic thresholds that are above the thresholds set by international standards. Certain issues arise when the power system's Hosting Capacity (HC) threshold reaches the system's hosting capability. In low-voltage distribution systems, the hosting capacity of PV systems is impacted by the Total Harmonic Distortion (THD) and Total Demand Distortion (TDD) levels. In this paper, the enhancement of hosting capacity has been achieved for the solar system in the distribution network. The proposed enhancement deals with a lot of considerations such as the capability current of the line and transformer, over and under voltage at the connection point of the distribution system and the PV system, known as the Point of Common Coupling (PCC), the limitation of total harmonic distortion, and line losses by using a new design of harmonic filter (high passive filter). Modeling of a PV system with grid-connected and passive harmonic filter has been validated based on a real-time Hardware in the Loop (HIL) OPAL-RT 4510 Powered by MATLAB SIMULINK. The new high-passive filter design leads to a remarkable 96.12% increase in the maximum hosting capacity (HC) of the system. Moreover, it brings about a reduction of 4.13% in the total harmonic distortion (THD) and 6.32% in the total demand distortion (TDD) of the system. In addition, it enhances the bus voltage by 0.98 pu, improves the power factor to 0.96, and reduces losses by 31.3%. In addition, the proposed technique has been compared to the previous technique.

INDEX TERMS Solar system, hosting capacity (HC), distribution network, harmonic distortion, high passive harmonic filter.

NOMENCLATURE

PV	Photovoltaic.
LV	Low-voltage.
HC	Hosting Capacity.
PCC	Point of Common Coupling.

The associate editor coordinating the review of this manuscript and approving it for publication was Tariq Masood.

TDD	Total Demand Distortion.
PQ	Power Quality.
DG	Distributed Generation.
DER	Distributed Energy Resources.
HF	Harmonic Filter.
DN	Distribution Network.
THD	Total Harmonic Distortion.
HIL	Hardware in the Loop.
FDHPF	Decoupled Harmonic Power Flow.
DSR	Distribution System Reconfiguration.
SLD	Single Line Diagram.
PQE	Power Quality Enhancement.
PF	Power Factor.
MPPT	Maximum Power Point Tracking.
PSO	Particle Swarm Optimization.
CO	Carbon Oxide.

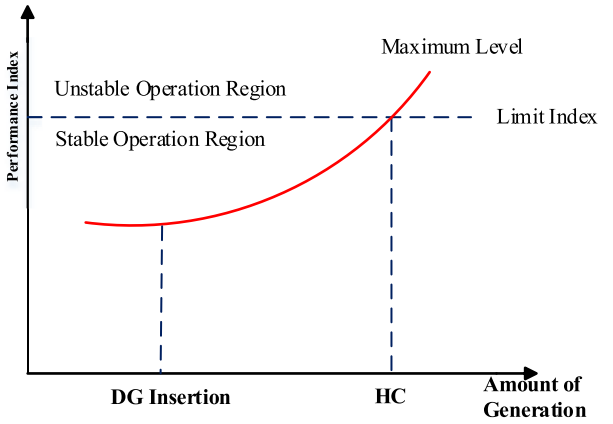

FIGURE 1. The concept of hosting capacity (HC) definition [10].

I. INTRODUCTION

In the past, generating electricity in the world resulted from fossil fuel consumption such as gas, oil, and coal which produce Carbon Oxide (CO_2) and Mono Carbon Oxide (CO) which affect climate change [1], also, the direction of power flow depend on unidirectional power flow from source to loads, increase the losses and increase the voltage drop. In terms of preserving the environment and using non-exhaustible resources, the world is directed to eliminate used fossil fuels by replacing or using sustainable energy sources like Photovoltaic (PV) systems and wind turbines, biomass, and hydropower [2]. PV has increased in the last years to share in the world's total capacity at the end of 2022 by 1019 GW [3], renewable energy changed the traditional power flow by enhancing the voltage profile and transmission losses. On the other side, the increase of the Distributed Generation (DG) power than the consumption of a local load produces negative impacts like overvoltage issues, overheating of equipment, reverse power flow, and damage to protective equipment. The term Hosting Capacity (HC) expresses the maximum power that can be added to the distribution electrical grid without any disruption to the system performance [4]. The boundary of the electrical system under HC has been shown in Fig.1.

The determination of the PV system integration capacity in low-voltage distribution networks depends on several factors including the characteristic of the feeder at the connected PV system, the level of the loading, and the nature of the PVs location connected with a grid [5]. They are several types of PV hosting capacity enhancement including inverter control that incorporates smart technology and utilizes a variety of control strategies, including active power control, reactive power control, power factor control, frequency control, and combined control [6]. The smart inverter control with a storage battery system has been used to improve the PVHC in a low-voltage distribution network. While this method is considered the best method in terms of performance, it is very expensive compared to other methods [7]. The second type of PV hosting capacity enhancement has been presented by using a harmonic filter to reduce the (THD) and the (TDD) where the effects of generation distortion of harmonics by DG unit on the HC in low voltage distribution grid have been studied [8], [9].

In [8], a passive harmonic filter has been designed to enhance the PVHC in low-voltage distribution systems depending on optimization problems by taking into account over and under-voltage issues, transmission line losses, a harmonic distortion produced by non-linear load (six-pulse rectifier), and the capability currents of the line. The results enhance the PVHC and increase the system's power factor by reducing THD and TDD. In [11], the HC and PF of the system at the (PCC) have been obtained. Furthermore, other parameters have been obtained such as the overall price of the passive filter, and the minimum total level of harmonic distortion in voltage and current by using Multi-Objective Firefly Algorithm (MOFA) based on Pareto optimization. In addition, a comparative study between the previous algorithm such as a comparison between Multi-Objective PSO (MOPSO) and Non-dominated Sorting Genetic Algorithm (NSGA-II) has been presented for similar objectives. while in 12, the authors investigate a new design in the harmonic filter known as the C-type of passive filter to enhance the HC in the distribution grid for electricity with a low voltage. The proposed method in this reference depends on reducing the level of distortion present in both current and voltage signals at a bus connected in renewable energy and obtaining the maximum HC based on a new optimization known as the (pb-MOBA) is a bat algorithm that utilizes the Pareto principle and is designed to optimize multiple objectives simultaneously. In [9], the Distribution System Reconfiguration (DSR) has been used to boost PV Hosting Capacity (PVHC). However, by combining multiple services, DSR is investigated in a multi-objective structure to enhance the voltage level, lessen the overall energy waste, and enhance PVHC.

To provide a more adequate evaluation of the objectives, stochastic demand scenarios are also incorporated

by using several amalgamations of linear and nonlinear loads. Ultimately, a solution approach by applying both the Non-dominated Sorting Genetic Algorithm II (NSGA-II) and a fuzzy decision-making method is suggested for the current multi-objective issue.

This paper presents a novel design of a passive harmonic filter connected at the load bus in conjunction with a PV system. The passive harmonic filter is employed to enhance the hosting capacity of the system. The results take various factors into account, including the limitations of over and under voltages in the system's voltage profile, the current capacity of the line, the power factor of the system, and the maximum limitations of total and individual harmonics. The results of passive harmonic filter elimination of THD, TDD, increase PF of the system. Furthermore, this study introduces the hosting capacity (HC) concept in a low-voltage distribution utility through the utilization of both simulation and Hardware-in-the-Loop (HIL) emulation. The PV systems, featuring Maximum Power Point Tracking (MPPT) and a boost converter, voltage source inverter, and utility grid, are modeled using OPAL-RT OP4510 HIL.

The remaining parts of this study can be organized as: After the part of the introduction, section II gives the understanding of the HC for the PV structure. In addition, the design of the passive filter, the PV model, and the parameters of the grid have been presented. Section III shows the results and comparative results with different types of passive filters. The final section, section IV, includes the conclusion and a discussion of future work.

II. PASSIVE FILTER DESIGN FOR HOSTING CAPACITY

In this section, understand the hosting capacity control, the proposed design in the passive filter, and the previous filter design.

A. HOSTING CAPACITY LITERATURE REVIEW

Modern distribution systems carry highly non-linear loads because the application of power semiconductor devices has increased in the power grid, hence the linear distribution system has no longer present. Distortion voltages in all buses and the feeder current are a direct consequence of increasing nonlinear loads [13]. Moreover, the worst case of harmonic distortion occurs when adding the Distributed Generation (DG). The reason is that the DG inserts harmonic current injection into the distribution network. Harmonic distortion is dangerous as it affects the time life of cables and malfunctions of industry devices and electronic drives [14]. To accurately measure overall PCC voltage and line current distortion of specific harmonic orders, standard indices must closely adhere to IEEE Standards 519 and 1547, both including and excluding DERs [15], [16].

It is worth noting that the integration of DG is assessed annually by dividing the total MW generated yearly ratio of DG impact by the total load profile over the same period, it is not entirely clear what is causing concern, but it seems that the focus is on the instantaneous aspect of the situation. References [17], [18], and [19] have also explained and verified how the increase in renewable energy penetration affects individual Power Quality (c) criteria, also, a simulated test distribution system was used to obtain data for formulating a composite index. The global figure shows the variations in THD present in the PCC voltages under the four-distribution system experimental conditions described. Fig. 2 shows the HC in four different cases in grid performance and DG unit. The harmonic increase in a grid and DG unit led to decreasing the HC in the system and a decrease in the power factor of the system. The restriction of hosting capacity for renewable energy is a low harmonic performance of a distribution network. Devices that improve Power Quality (PQ), which may provide reactive power regulation and harmonic reduction, are essential for boosting distributed grids' capacity to host new users [20]. Recently moving towards enabling DG units to carry out many tasks, such as harmonic load reduction, reactive power support, and actual power injection, to boost independence in prospective DG systems. The harmonic filters used to enhance the HC in low voltage distribution utility, are various types of harmonic filters such as active, passive, and hybrid filters system. The HC increases when using harmonic filtering as demonstrated in Fig. 3. The enhancement has been done based on Power Quality Enhancement (PQE) equipment, those devices supply the reactive energy control and harmonic compensation to find the significate role to improve the hosting capacity in power system [21]. The constraints of hosting capacity in a low-voltage distribution grid, such as overvoltage, undervoltage, line current capacity, and transformer limitations, are described in [4], [22], and [23].

B. HOSTING CAPACITY CONTROL METHODS

Because of the hosting capacity, it means the acceptance of penetration level in Distributed Generation (DG) without any one of the performance indices changing or exceeding the maximum level of the power system. The performance indices work as a limitation of distributed generation systems when tied to the utility at a low voltage distribution system, while the importance of performance indices increases when using DG units in a renewable energy system. That is why the hosting capacity should be improved when the system is linked to renewable energy in low-voltage distribution networks [24]. Fig 4. demonstrates the categorization of crucial indicators of the system that generally constrain the extent of renewable power penetration. It is worth noting that it should be reiterated that all the performance variables are regarded as limits in the current HC improvement dilemma.

The voltage level at the bus must fall within a specific range, as defined by global standards, throughout the distribution system. Moreover, when there is distributed generation, identical requirements must be observed [25].

The highest level of renewable energy integration and the overvoltage issue that occurs can be studied for the system

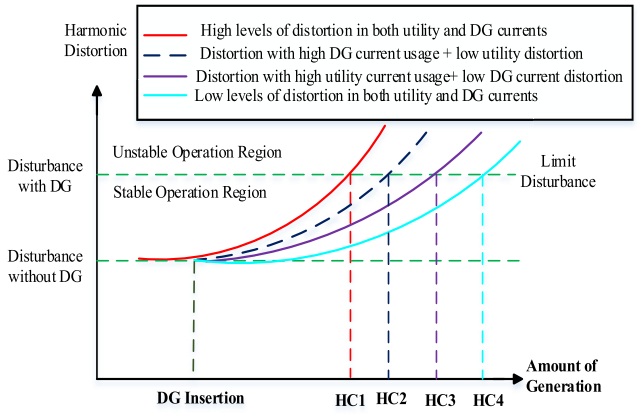

FIGURE 2. The principle of HC in four different cases [11].

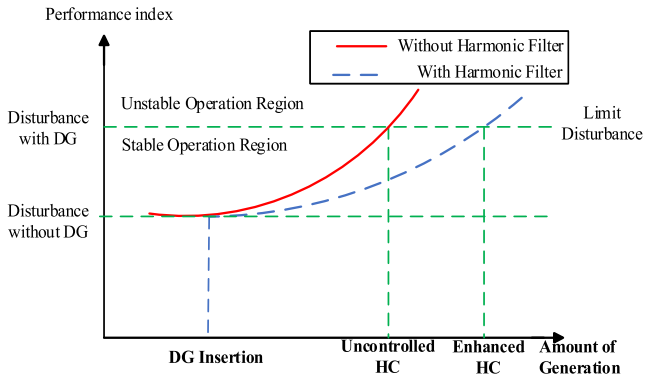

FIGURE 3. The key of HC enhancement with using harmonic filter [21].

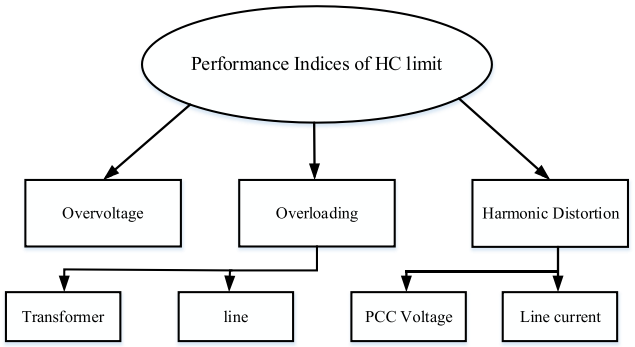

FIGURE 4. The categorization of system performance indices that limit the HC [5].

shown in Fig. 5. Where the Single Line Diagram (SLD) includes two buses (generation bus and load bus) With the integration of DG and load [26]. The increase in voltage at the PCC is described in Equation 1: [26].

$$\Delta V = VR - VS = \frac{P_d * R + Q_d * X}{|V_s|} + j\frac{P_q * X - Q_q * R}{|V_S|} \cong \frac{P * R + Q * X}{|V_S|} \quad (1)$$

where V_S is the normal voltage at the generation bus, V_R is the voltage at the end bus or load bus, ΔV is the voltage rise of the system when connected DG unit, R and X represent the resistance and reactance equivalent of the transmission line and transformer, respectively, the P is real power to injected a system, and Q the reactive power can be either injected or absorbed from the system depending on the voltage cases.

From equation 1, the problem of voltage rise (ΔV) depends on several parameters such as the generation bus voltage (V_S), term P^*R and Q^*X, the voltage in the slack bus is controlled by several types such as on-load tap changer transformer (substation transformer) or the cable reinforcement its means that changing the cables with a thicker one, when the cross-section area of the cables increases that reduce the cable's impedance elements (R and X), hence increase the current capability of the line. In addition, it solves the voltage rise problem. Hence the system's HC would be increased, but the method (cable reinforcement) is not economical because it is very extensive. Another solution by reactive power control based on a smart inverter has been presented, where the reactive power at PCC has been absorbed and injected by the smart inverter to reduce the overvoltage occurrence and prevent Undervoltage [27]. Active power control is also used to decrease the overvoltage issue by using a storage system [28]. It is worth noting that selecting the best solution could be influenced by other parameters like the (Q/P) or (X/R) ratios.

The primary aim of this paper is to enhance the HC, depending on using a passive filter. So, two major objectives have been presented:

(1) Analysing the hosting capacity of distorted distribution networks and demonstrating how harmonic distortion affects it while considering grid voltage asymmetry, harmonic currents produced by DG, and different degrees of load nonlinearity.

(2) using a harmonic filter such as a passive filter type to improve the HC of low voltage distribution systems.

C. TWO-BUS DISTRIBUTION NETWORK

The two-bus distribution network has been chosen to be the system under the hosting capacity study as shown in Fig. 6. The main reason for choosing the two-bus distribution network is that it has several components which include several devices and parameters like a group of loads (linear and non-linear load), PV solar system, passive filter harmonic, transmission line, and transformers. One of the frequently encountered non-linear loads are the six-pulse rectifier. Many publications choose this system with filter size optimization to validate the effect of harmonic and how to eliminate it [29], [30].

In this paper, a novel passive design has been presented to enhance the HC of PV systems in low-voltage distribution networks by using the Fast Decoupled Harmonic Power Flow (FDHPF). In the FDHPF method, the flow of power computation is done separately rather than concurrently for each order harmonic after decoupling all the harmonics. Using nodal analysis, the single-phase equivalent circuit for the PV

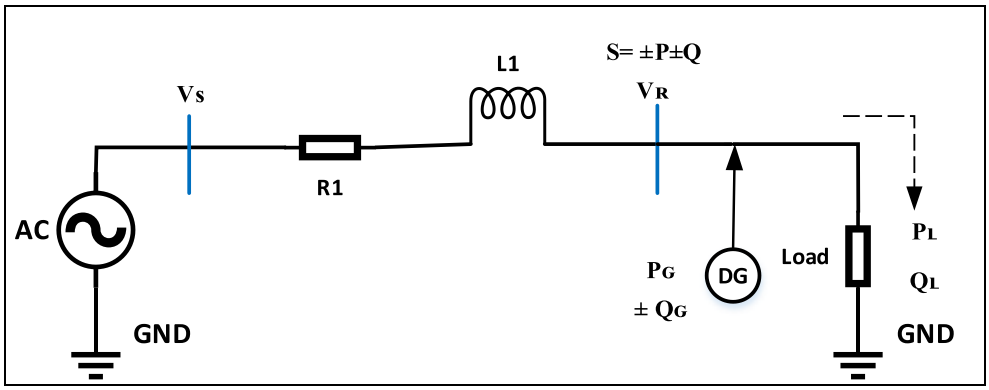

FIGURE 5. The system representation by using two buses with connected DG unit integration.

system connection can be solved for the voltage at the PCC and the current in the transmission line at the fundamental frequency, harmonic filter, and A combination of linear and non-linear loads are demonstrated in Fig.7. After determining the voltage at PCC and line current in fundamental components, the same technique determines the harmonic frequency components for voltage at PCC and the current in the line.

The grid has been set to be a reference bus or slack bus $V_s\,(h)$ and the harmonic order in voltage at the reference bus is demonstrated in Equation 2 [11].

$$V_s\,(h) = C\,(h) * V_s(1) \tag{2}$$

where, $C(h)$ is a factor that varies with the degree of harmonic distortion in the utility grid,

$V_S(1)$ is the essential component's voltage in the utility grid.

The transmission line impedance $Z_L(h)$ in h^{th} order harmonic can be expressed in equation 3 [11].

$$Z_{\mathrm{L}}(h) = R_{\mathrm{L}}(h) + JX_{\mathrm{L}}(h) = \sqrt{(R_{\mathrm{L}}(h))^2 + (X_{\mathrm{L}}(h))^2} \tag{3}$$

where, $Z_L(h)$ is the transmission line impedance h^{th} number of order harmonic, $R_L(h)$ and $X_L(h)$ are the transmission line resistance and reactance respectively at h^{th} frequency of the harmonic order, moreover, $R_L(1)$ and $X_L(1)$ are the transmission line resistance and reactance at the system's fundamental frequency. The parameters of the line depend on the frequency where the eddy currents and skin effects exist [31], [32].

The linear load consists of a series of resistance as well as an inductor. where a resistor is consumed the real power and an inductor is consumed the reactive energy are illustrated in Fig. 5 and Fig. 6. The active power of linear load and reactive energy is represented P_L and Q_L sequence, then the resistance of linear load and reactance at h^{th} order harmonic frequency are denoted by letter $R_L(h)$ and $X_L(h)$ are demonstrated as follows [8]:

$$R_L(h) = \frac{P_L}{|I_L(1)|^2} \tag{4}$$

$$X_L(h) = \frac{Q_L}{h|I_L(1)|^2} \tag{5}$$

$$I_L(h) = \frac{V_{S2}(h)}{R_L(h) + jX_L(h)} \tag{6}$$

where, $I_L(1)$ is the basic frequency element of linear load current at PCC.

A current source is represented by the non-linear load of the framework [33]. If the real energy of the non-linear load is denoted by P_{nl} and reactive energy usage in the non-linear load is denoted by Q_{nl}, hence the basic component and hth harmonic of a specific order of the non-linear load are $\mathrm{I_{nl}}(1)$ and $\mathrm{I_{nl}}(\mathrm{h})$ respectively are demonstrated in equations 7 and 8 are shows follow [11].

$$I_{nl}\,(1) = \frac{P_{nl} + Q_{nl}}{V_{s2}\,(1)} \tag{7}$$

$$I_{nl}(h) = M(h) * I_{nl}(1) \tag{8}$$

where, $V_{s2}\,(1)$ is the basic parameter of the secondary voltage of the distribution transformer or the fundamental voltage component at PCC, $M(h)$ is a constant value or the proportion of the hth order harmonic to the fundamental element of non-linear load current and determine by using Experimental evaluation in a real-world setting and using Fourier series assessment of customer load devices.

The PV system is like the non-linear load represented current source in the structure [34], but the difference between non-linear load is that injected active power does not absorb active power like non-linear load, and lets the PV system produce real energy only at the basic frequency. If $\mathrm{S_{PV}}$ is the MVA of the PV system hence determine the fundamental current $I_{PV}(1)$ and the hth order distortion of harmonic $I_{PV}(h)$ of the PV model are demonstrated in equations 9 and 10 [8].

$$I_{PV}\,(1) = \frac{S_{PV}}{V_{s2}\,(1)} \tag{9}$$

$$I_{PV}(h) = \beta(h) * I_{PV}(1) \tag{10}$$

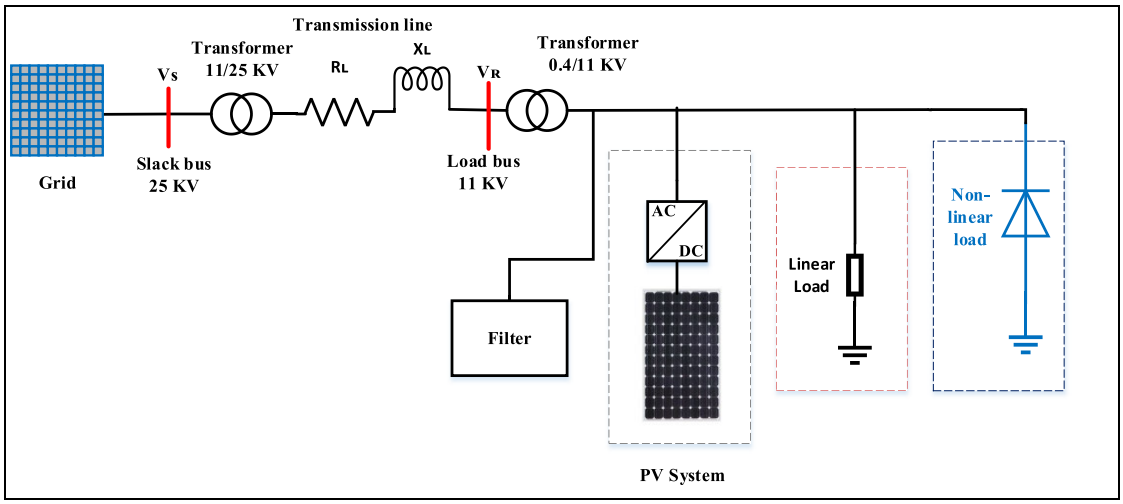

FIGURE 6. The structure of studied PV power system model.

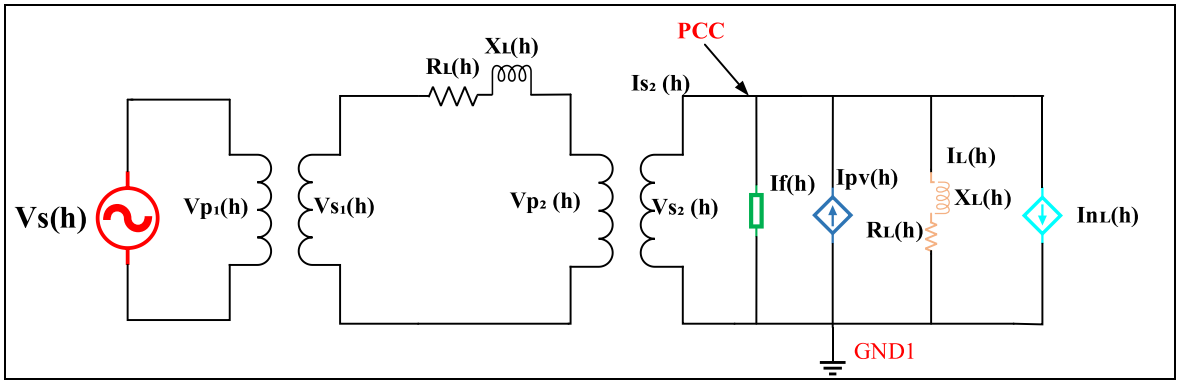

FIGURE 7. The configuration of SLD for grid-connected PV system under study.

where $\beta(h)$ is the proportion of the h[th] order harmonic to the active component of PV Solar structure current.

The percentage of a non-linear load of the system K_N can be calculated by the amount of actual power or reactive energy of non-linear load divided by the total loads (linear and non-linear) of the system as [8]:

$$K_N = \frac{P_{nl}}{P_{nl} + P_l} = \frac{Q_{nl}}{Q_{nl} + Q_l} \tag{11}$$

where, K_N is known as the percentage of non-linear loads of the system.

D. PROPOSED PASSIVE HARMONIC FILTER CONFIGURATION

Fig.8 shows a single-line diagram of a new design in a high-pass filter. The filter Reworded: Comprises the primary capacitance (X_{C1}) in sequence with the parallel of a combination of two branches, branch one consists of capacitance (X_{C2}), and the second branch is consisted of inductive reactance (X_L) and internal resistance of the inductor (R_1). The equivalent impedance of the high pass filter of the system is illustrated as (12)–(14), shown at the bottom of the next page, [11].

The secondary current of the distribution transformer From Fig 7. ($I_{S2}(h)$) is equal to the sum of filter current, PV system current, and linear and non-linear currents [11].

$$I_{S2}(h) = I_F(h) - I_{PV}(h) + I_L(h) + I_{nl}(h) \tag{15}$$

$$V_{S1}(h) = V_{P1}(h) * \frac{N_{S1}}{N_{P1}} \tag{16}$$

$$I_{S1}(h) = \frac{V_{S1}(h) - V_{p2}(h)}{R_L(h) + jX_L(h)} \tag{17}$$

$$I_{S2}(h) = \frac{V_{S(h)*\frac{N_{S1}}{N_{P1}} - V_{P2}(h)}}{R_L(h) + jX_L(h)} * \frac{N_{P2}}{N_{S2}} \tag{18}$$

The final equation of order harmonic components of secondary current $I_{S2}(h)$ represented as [11]:

$$\frac{V_{S(h)*\frac{N_{S1}}{N_{P1}} - V_{P2}(h)}}{R_L(h) + jX_L(h)} * \frac{N_{P2}}{N_{S2}} = \frac{V_{S2}(h)}{Z_F(h)} - \beta(h) * I_{PV}(1) + \frac{V_{S2}(h)}{R_L(h) + jX_L(h)} + M(h) * I_{nl}(1) \tag{19}$$

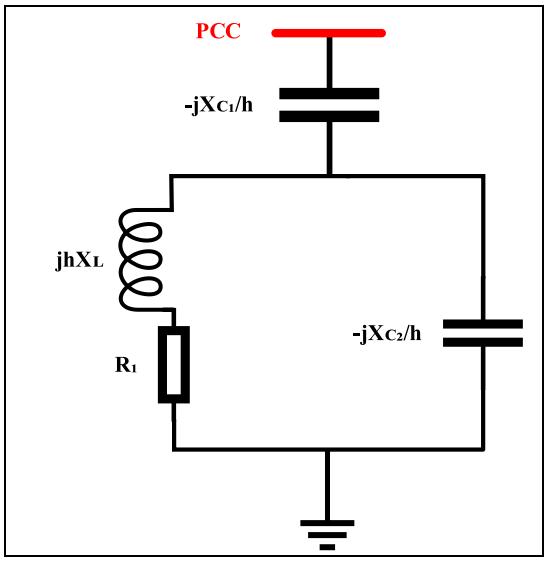

FIGURE 8. The equivalent diagram of high pass filter circuit.

The passive harmonic filter at PCC has been designed to obtain the highest level of system penetration possible without changes to the typical functioning of the system. The mathematical equation of HC can be defined from equation (20) [35].

$$HC(\%) = \frac{P_{PV}}{S_{rated}} * 100 \tag{20}$$

where, P_{PV} is the amount of solar PV generation, and S_{rated} is the rated apparent power of the load bus.

The system's hosting capacity is limited by several performance indices such as voltage limits at the connected bus, limits of THD in voltage and current, capability of line current, the capacity of maximum PV system linked at load bus, and the range of power factor limits which can be summarized as:

1) LIMIT OF VOLTAGE BUS

the voltage bus at PCC has been constrained by two values the lower value equals 0.95 pu and the uppermost value equals 1.05 pu [36], [37], the rms value of electric potential difference constraints can be presented as:

$$0.95 \leq \sqrt{\sum_{h=1}^{h=\infty} V_{S2}(h)} \geq 1.05 \tag{21}$$

TABLE 1. Maximum individual order harmonic of current accordance with IEEE Std.519 [15].

Harmonic order	IHDC%
h <11	7
$11 \leq h < 17$	3.5
$17 \leq h < 23$	2.5
$23 \leq h < 35$	1
$35 \leq h$	0.5

2) TOTAL HARMONIC DISTORTION (THD)

According to the IEEE Std.519 [38], the overall voltage harmonic distortion at PCC maximum reaches 5%, the equation of THDV is described in equation (22) as:

$$THDV(\%) = \frac{\sqrt{\sum_{h=2}^{\infty} |V_{S2}(h)|^2}}{V_S(1)} \leq 5\% \tag{22}$$

3) TOTAL DEMAND DISTORTION (TDD)

the index is employed to evaluate the harmonic characteristics of transmission cables in the presence and absence of (DGs). The allowable TDD (Total Demand Distortion) in a system is limited by IEEE Std. 519 and is determined based on factors such as the highest current demanded by the load (I_{s2}), fault threshold, as well as the type of DG framework, such as distributed generation, grid distribution generating devices, or a customer network [36]. The percentage of TDD in the system does not increase more than 8% as described in the equation (23).

$$TDD(\%) = \frac{\sqrt{\sum_{h=2}^{\infty} |I_{S2}(h)|^2}}{I_{S2}(1)} \leq 8\% \tag{23}$$

4) INDIVIDUAL TOTAL HARMONIC DISTORTION

Following IEEE Std.519, the individual order harmonic of voltage at PCC does not increase than 3% at operating voltage less than or equal to 69 kV. The harmonic of each specific order of the current is restricted to various values as demonstrated in Table (1). The equations (24 and 25) describe the individual voltage and current respectively.

$$IHDV(\%) = \left[\left| \frac{V_{S2}(h)}{V_{S2}(1)} \right| \right] \leq 3\% \tag{24}$$

$$IHDC(\%) = \left[\left| \frac{I_{S2}(h)}{I_{S2}(1)} \right| \right] \leq according\ table\ (1) \tag{25}$$

$$Z_F(h) = -j\frac{X_{C1}}{h} + \frac{-j\frac{X_{C2}}{h} * (R_1 + jhX_L)}{R_1 + jhX_L - j\frac{X_{C2}}{h}} \tag{12}$$

$$Z_F(h) = \frac{-jh * X_{C1}(h * R_1 + jh^2 * X_L - jX_{C2}) - jh * X_{C2}(R_1 + jh * X_L)}{h^2 * R_1 + jh^3 X_L - jh * X_{C2}} \tag{13}$$

$$I_F(h) = \frac{V_{S2}(h)}{Z_F(h)} \tag{14}$$

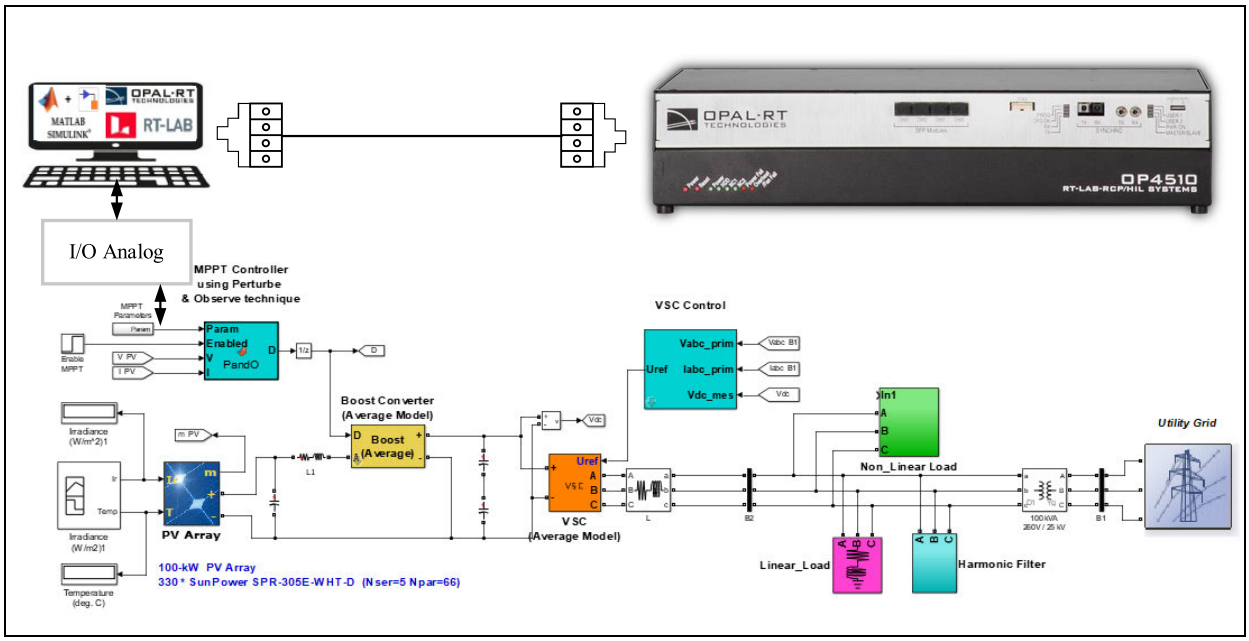

FIGURE 9. Hardware in the loop validation by OPAL-RT 4510 for the system model setup.

TABLE 2. The harmonic current of non-linear load.

Number of Harmonic	5	7	11	13	17	19	23	25	29
Amplitude%	23.77	8.76	6.92	4.11	2.65	2.13	0.82	0.92	0.27

TABLE 3. The current harmonic content of the PV system depends on the DG unit.

Harmonic order	Amplitude%	Harmonic order	Amplitude%
2	0.012	12	0.003
3	0.06	13	1.498
4	0.006	14	0.003
5	0.72	15	0.009
6	0.003	17	0.822
7	3.012	18	0.003
8	0.003	19	0.644
9	0.02	21	0.006
11	2.384	23	0.221

TABLE 4. The harmonic voltage of the utility grid.

Harmonic order	5	7	11	17	19	23	25	29
Magnitude (%)	3	2	2	1	1	1	0.5	0.5

5) CAPABILITY OF LINE CURRENT

Harmonic Derating Factor (HDF) or the line's capacity to carry current shouldn't be greater than 100% about distorted line/cable currents [39].

$$HDF(\%) = \frac{1}{\sqrt{1 + \sum_{h=2}^{\infty} \left(\frac{R_L(h)}{R_L(1)}\right) \left|\frac{I_{S1}(h)}{I_{S1}(1)}\right|^2}} * 100 \leq 100\% \tag{26}$$

6) POWER FACTOR (PF) RANGE

the quality of power transfer increase from source to load when the PF at PCC with a limit of range minimum and maximum [30] is expressed in equation (27).

$$PF = \frac{P}{S} = \frac{\sum_{h=1}^{\infty} P(h)}{\sum_{h-1}^{\infty} S(h)} \tag{27}$$

$$\text{where, } 0.9 \leq PF \leq 1 \tag{28}$$

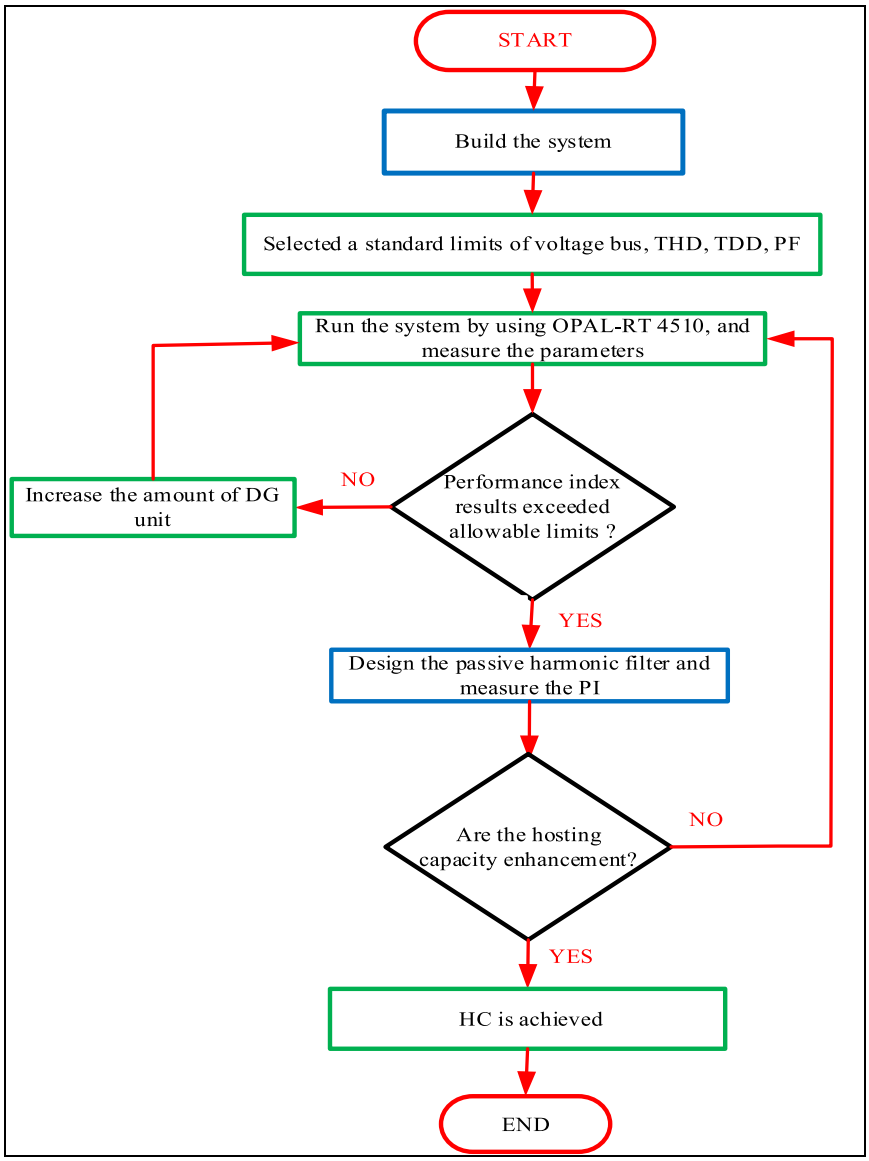

FIGURE 10. Flowchart of PV studied system in OPAL-RT 4510 based on filter design.

TABLE 5. Results of the system absence connected DG unit.

Elements	Magnitude
Bus voltage at PCC	0.96
THD in voltage at PCC	13.15%
TDD of the line is current	12.21%
PF at PCC	0.81
The power dissipated by the system	984.9 w

III. MODEL SETUP FOR HARDWARE IN THE LOOP REAL-TIM

The system consisted of a PV array, MPPT controller using Perturb & Observe (P&O) technique, DC/DC boost converter, Voltage Source Inverter (VSI), linear load, non-linear load, harmonic filter, distribution transformer, and the utility grid. These modules have been built and downloaded to OPAL-RT 4510 which is shown in Fig.9. The utilization of passive harmonic filters and OPAL-RT 4510 for harmonic compensation (HC) of the system is demonstrated in Fig. 10's flowchart. The initial step in the flowchart involves building a model on OPAL-RT 4510. Next, standard limits are selected based on IEEE.Std.519 for various parameters such as bus voltage, THD, TDD, and PF. Once the constraints

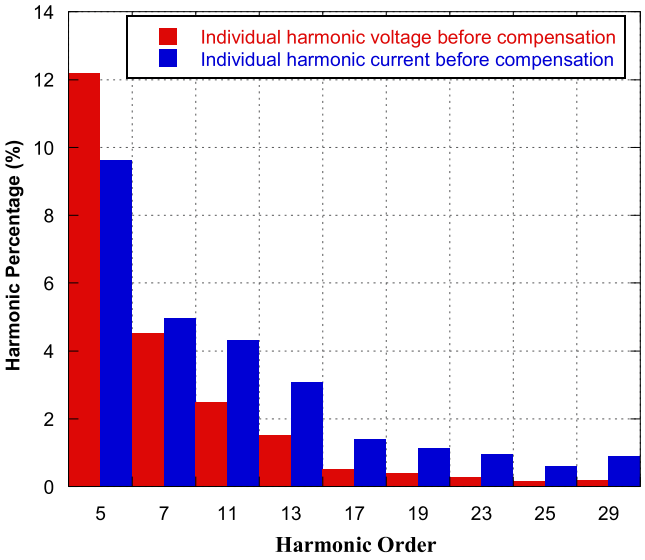

FIGURE 11. Individual order harmonic voltage and current before compensating.

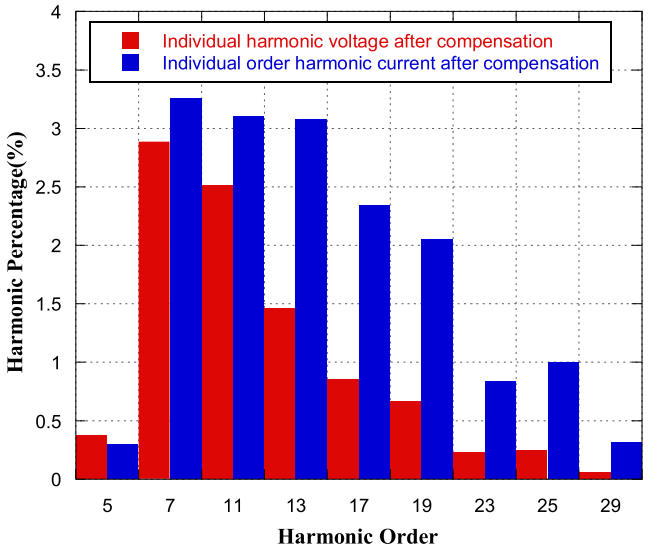

FIGURE 12. Individual order harmonic voltage and current after compensating.

are determined, the system is run, and its performance is measured. If any performance parameters exceed the standard limits, a passive harmonic filter is built to improve the HC and performance parameters.

IV. SIMULATION RESULTS

Within this part, first, study the HC in a low voltage distribution network by using a new design of the passive harmonic filter and displays the circuit parameters of the arrangement. Second, comparing the recommended method with previous work.

A. MATLAB SIMULATION RESULTS

The study system demonstrated in Fig. 6, composed of a utility with an operating voltage equal to 25 kV, a step-down transformer (25/11 kV), the resistance and reactance of the transmission line are equal to 0.0754 Ω and 0.0943 Ω respectively, and load bus is connected on several components such as 100 kW of PV system, 130 kVA linear loads, 100 kVA non-linear loads, and passive harmonic filter. The non-linear loads contained in the harmonic current spectrum are demonstrated in Table (2). Table (2) describes the worst-case scenario for the harmonic current of a non-linear load in the harmonic order of 5, which is equal to 23.77%. In addition, according to IEEE Std. 519, the individual order harmonic of current does not increase by more than 7% when the order of the harmonic is less than 11. Furthermore, the order of the harmonic from 11 to 17 does not increase by more than 3.5%. Moreover, the PV system has a harmonic current range described in Table (3), The harmonic current of a PV system does not exceed the standard individual order harmonic current limit. However, the worst individual order harmonic in a PV system, which occurs in the harmonic order of 7, is equal to 3.012%,

TABLE 6. Results of the system after connecting the DG unit and filter compensation.

Parameter	Value
Filter Parameters (X_{C1}, X_{C2}, X_L, R)(6.72, 26.5, 0.268, 0.01) Ω	
Bus voltage at PCC	0.98
THD in voltage at PCC	4.13%
TDD of the line is current	6.32%
PF at PCC	0.96
The power dissipated from the system	334.01 W
Penetration level	99.39 kW
Hosting capacity	96.12%

TABLE 7. Results of the system after connecting the DG unit and filter compensation by using real-time simulation.

Parameter	Value
Filter Parameters (X_{C1}, X_{C2}, X_L, R) (6.72, 26.5,0.268, 0.01) Ω	
Bus voltage at PCC	0.995 pu
THD in voltage at PCC	4.583%
TDD of the line is current	7.1 %
PF at PCC	0.974
The power dissipated off the system	337. 2W
Penetration level	101.5 kW
Hosting capacity	97.5%

and the harmonic voltage spectrum of the grid side according to IEEE.Std.519 is illustrated in Table (4).

The result of the system without a PV solar system is shown in Table (5), It is noticeable that the voltage at the connected bus is 0.96 pu, and the amount of THD in voltage at the PCC exceeds the IEEE Std. 519 criterion states that the THD in the system's voltage should not exceed 5%. Additionally, the TDD of the line current in the system is 12.21%, which is higher than the IEEE Std. 519 standard of 8%. Moreover, the PF of the system is low compared to the standard for power

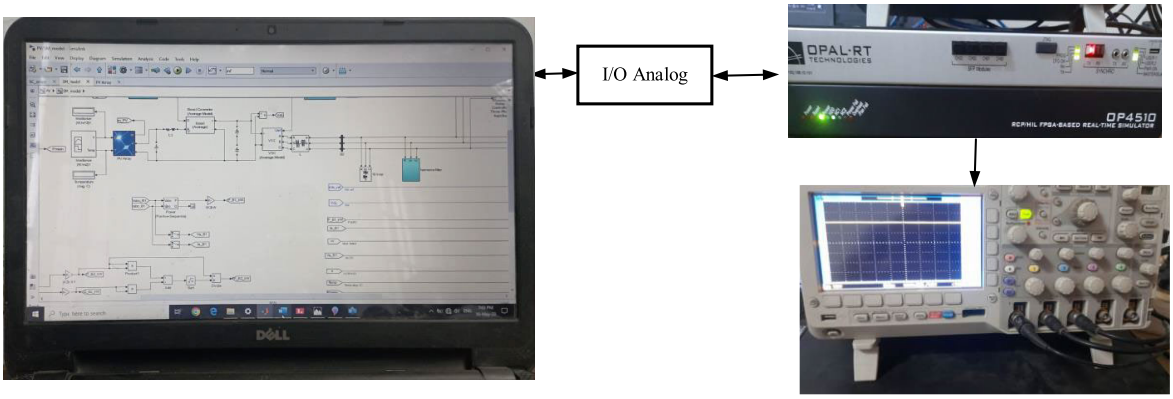

FIGURE 13. The studied system setup in OPAL-RT 4510.

TABLE 8. Comparative study between the proposed method and previous works.

Parameter				
Filter Parameters (X_{C1}, X_{C2}, X_L, R)		(6.72, 26.5, 0.268, 0.01) Ω		
method	Uncompensated	Ref [8]	Ref [11]	Proposed
Bus voltage at PCC	0.96 pu	1.02	0.98	0.98
THD in voltage at PCC	13.15%	19.68%	5.35%	4.13%
TDD of the line is current at	12.21%	17.52%	7.62%	6.32%
PF at PCC	0.81	0.92	0.95	0.96
Power losses of the system	984.9 W	338.61 W	335.77 W	334.01 W
Penetration level	-------	98 kW	99.29 kW	99.39 kW
Hosting capacity	------	92.5%	95.26%	96.12%

factor, and the transmission line losses are significant, measuring 984.9 watts. The current and voltage harmonic content for each frequency component at PCC without a connected PV system is demonstrated in Fig. 11. The current and voltage harmonic content for each frequency component exceed the limits specified by IEEE Std. 519. Specifically, the individual order harmonic voltage measures 12.2% for harmonic order 5 and 4.2% for harmonic order 7, in compliance with IEEE Std. 519, the individual order harmonic of voltage does not increase by more than 3%, and the individual order harmonic current measures 9.82% for harmonic order 5 and 4.5% for harmonic order 7, according to IEEE Std. 519, the individual order harmonic of current does not increaseby more than 7% when the order of the harmonic is less than 11.

The results of the system at PCC, after connecting the PV system and a high passive harmonic filter, are presented in Table 6. The HC of the system improves by 96.12%, and the power factor at PCC reaches 96 lagging. Line losses are reduced by 66.1% when compared to the system without the filter and PV system. Additionally, the THD decreases by 68.6% and the TDD by 48.2% when using a passive filter and a connected PV system, and the power factor increases by 20.99%. Fig. 12 illustrates the individual harmonic current and voltage at PCC with the connected PV system and high passive harmonic filter. The individual harmonic orders in voltage (5, 7, 11, 13, 17, 19) have values of 0.374%, 2.885%, 2.516%, 1.462%, 0.86%, and 0.663%, respectively. Similarly, the individual harmonic orders in current (5, 7, 11, 13, 17, 19) have values of 0.3%, 3.261%, 3.1%, 3.08%, 2.34%, and 2.05%, respectively. It is worth noting that the individual harmonic current and voltage do not exceed the individual standard harmonic.

The filter built with the connected solar system is used to enhance the HC of the PV system in low voltage distribution systems, decrease the THD of voltage and current, enhance the power factor of the system, maintain the voltage profile within limits, decrease the line losses of the system, and increase the efficiency within the system.

B. REAL-TIME OPAL-RT RESULTS

The studied system setup in OPAL-RT 4510 is shown in Fig. (13). The results of real power, power factor at PCC, voltage bus, line losses of the system, and THD in voltage and current are demonstrated in Fig.14, and Table 7. Fig.14 (a) demonstrated the real energy generated from the solar arrays at PCC. The real power produced from the PV solar system remains constant as it is not affected by any dynamic changes such as temperature, irradiance, and shading systems. The value of the active power generated is 101.5 kW. Fig.14 (b) shows the PF of the system at PCC. The PF of the system improves when using a high passive filter and reaches 0.974 lagging. Fig.14(c) illustrated the transmission line losses, when using real-time simulation, the losses of the transmission line increase by 0.955% compared to MATLAB

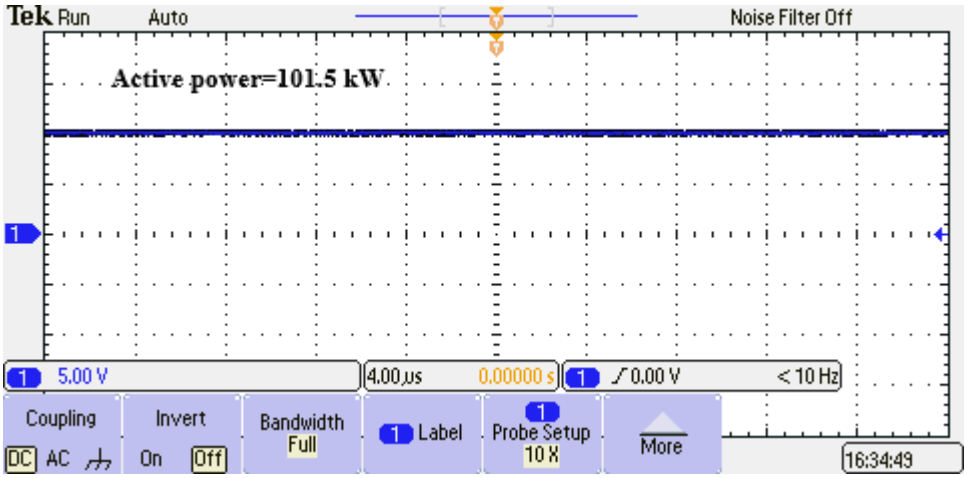

(a)

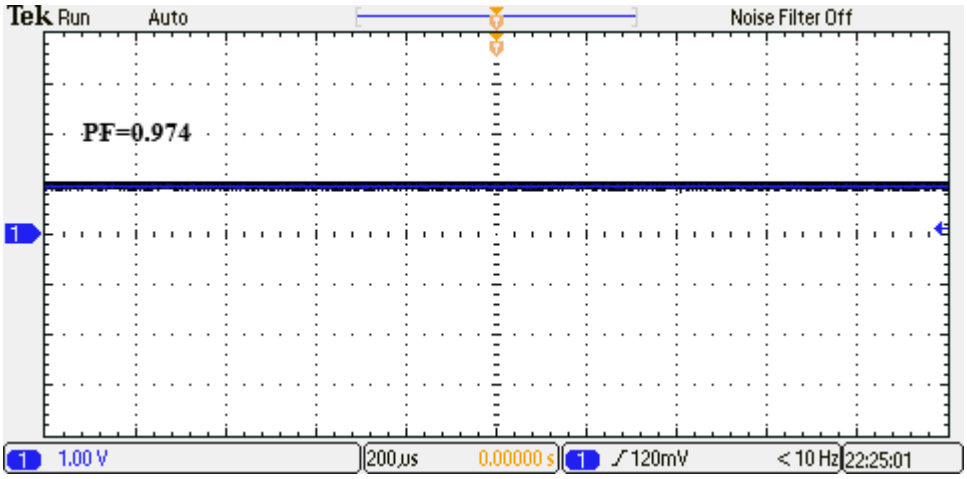

(b)

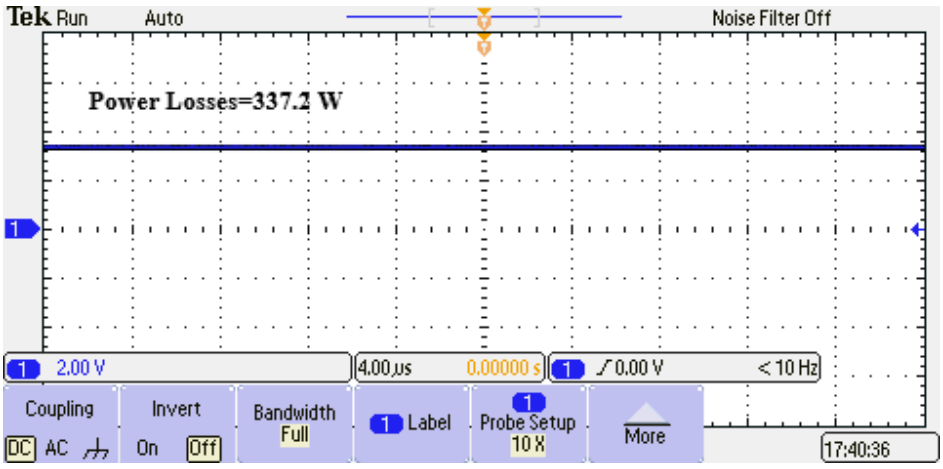

(c)

FIGURE 14. Outcomes in real-time simulation (a) real power (b) PF (c) power losses (d) THD at PCC (e) TDD at PCC (f) voltage bus.

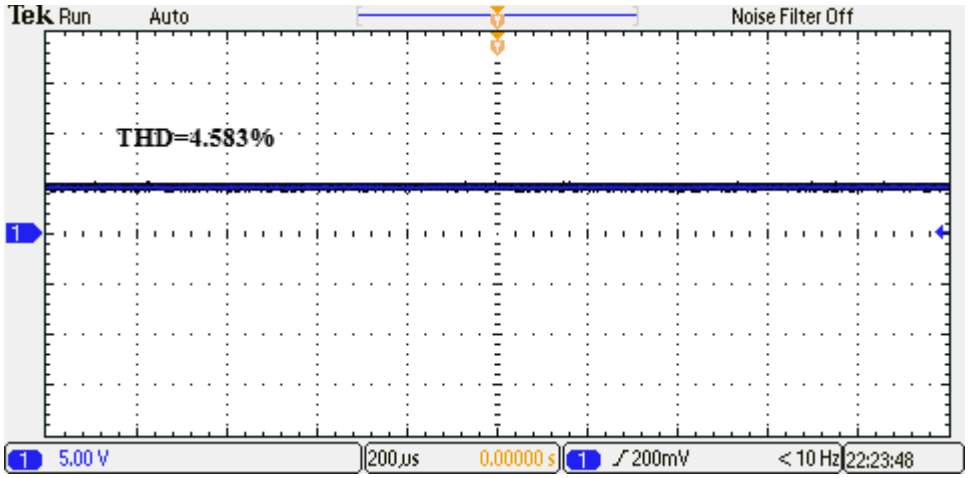

(d)

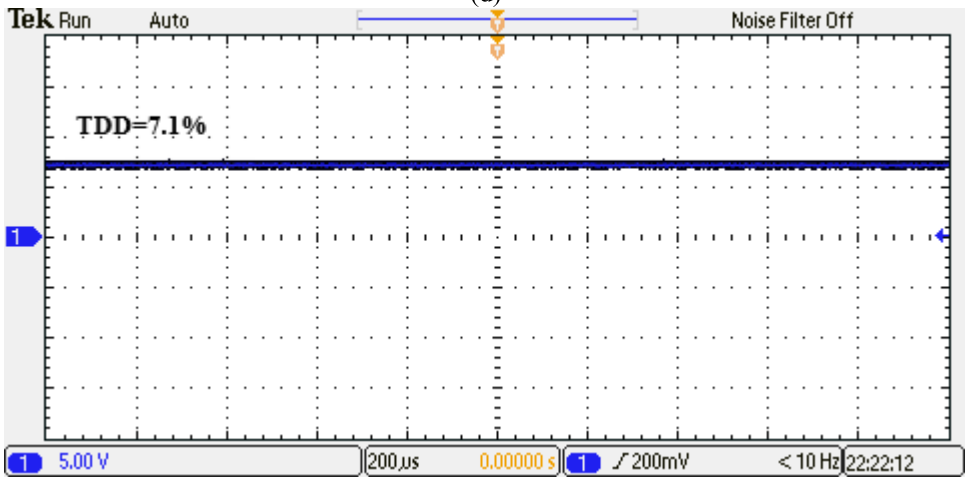

(e)

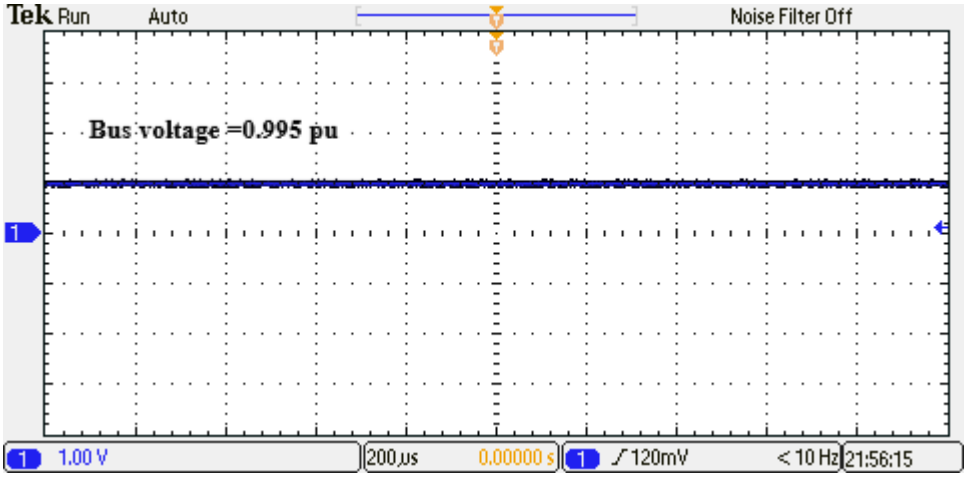

(f)

FIGURE 14. *(Continued.)* **Outcomes in real-time simulation (a) real power (b) PF (c) power losses (d) THD at PCC (e) TDD at PCC (f) voltage bus.**

Simulink. Fig.14 (d) explains total harmonic distortion in voltage, the THD of the system increases by 10.96% when using real-time simulation but does not exceed the standard limit of THD, the system remains fixed all the time as it is not affected by any dynamic changes during its operation. Fig.14 (e) shows the total demand distortion in line current,

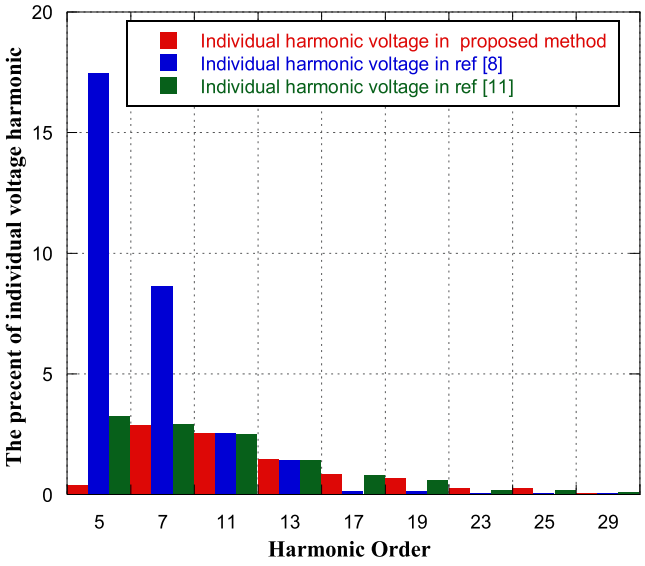

FIGURE 15. Individual order harmonic voltage in the proposed method and previous work.

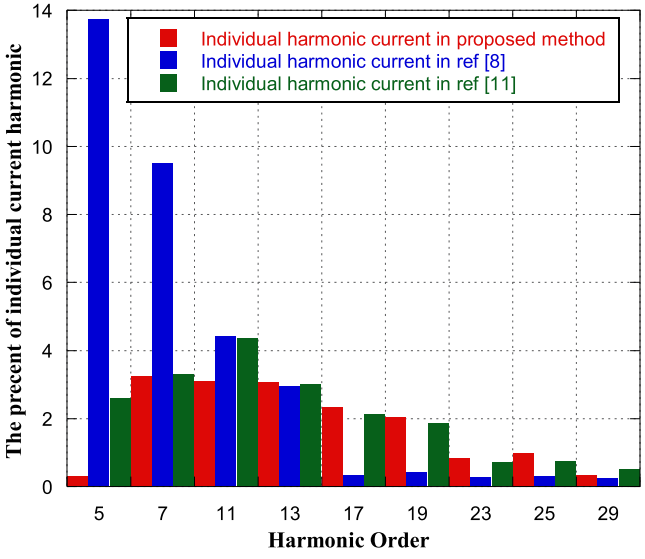

FIGURE 16. Individual order harmonic current in the proposed method and previous work.

the TDD of the system increases by 12.34% when using real-time simulation but does not exceed the standard limit of TDD, the system remains fixed all the time as it is not affected by any dynamic changes during its operation, and Fig.14 (f) demonstrated the line voltage at PCC, The distortion of the line voltage in the system is expressed by the voltage harmonic content. The bus voltage has a value of 0.995 pu, which does not exceed the voltage standard limit.

When comparing the results from MATLAB SIMULINK and REAL-TIME SIMULATION are shown in table 5 and 6, it noted that the active power increase, PF of the system increased, and HC of the system also increased, but the drawback losses and total harmonic distortion increase. The real-time simulation is more accurate than the MATLAB SIMULINK.

C. COMPARATIVE STUDY

The proposed method is evaluated against different previous methods, and it is observed that when the same design is used in the passive harmonic filter or C-type passive filter as described in [8], the hosting capacity decreases by 3.91% compared to the proposed method. Furthermore, the power factor at PCC reduces by 4.35% compared to the proposed method, and the line losses increase by 1.36%. In addition, the THD in voltage and current increases by 79.01%, and the TDD in the system increases by 63.93%. Furthermore, when comparing the proposed method with a new design of the passive harmonic filter known as the third-order damped filter in [11], it is observed that when the same design is used in the third-damped filter in the system, the HC in the low voltage distribution utility decreases by 0.9%. The losses are increased by 0.52%, and the THD and TDD in the system are increased by 22.8% and 17.1%, respectively. Additionally, the PF of the system at PCC is reduced by 1.05%. The comparative study between the proposed method and [8] and [11] is shown in Table 8. Moreover, the individual order harmonic voltage and current in the proposed method with comparing the previous work are demonstrated in Fig.15 and 16, respectively. It is observed that the individual order harmonic voltage and current in the proposed method are less than those observed in the previous work.

V. CONCLUSION

In this paper, the enhancement of HC in a low voltage distribution utility of a distorted distribution system with a connected PV system by using a high passive filter based on MATLAB SIMULINK and REAL-TIME SIMULATION (OPAL-RT 4510) has been achieved. The proposed technique takes into consideration over and under voltage fluctuations limits at PCC, losses of transmission line, power factor of the system, capability of the line current, voltage, and current harmonic content, both individually and in total, of the system.

A new design of the high passive filter enhances the maximum HC of the system by 96.12%, Moreover, it reduces the harmonic of the system in THD by 4.13% and TDD by 6.32%. in addition. It enhances the voltage bus by 0.98 pu. Also, it is accompanied by an improvement in the power factor to reach 0.96 and reduces the losses by 31.3%.

The comparative study between the proposed filter and the previous filters was conducted by evaluating their effectiveness in reducing voltage total harmonic distortion, minimizing transmission losses, and maximizing power factor. The suggested filter design methodology achieves a higher hosting capacity. Additionally, when dealing with high-power applications and significant levels of harmonic distortion, passive filters can be designed to achieve the goal of maximizing the hosting capacity as their primary objective function.

The result in real-time simulation is actual results compared with MATLAB Simulink, hence the results of the real-time simulation are more accurate.

REFERENCES

[1] S. Paraschiv and L. S. Paraschiv, "Trends of carbon dioxide (CO_2) emissions from fossil fuels combustion (coal, gas and oil) in the EU member states from 1960 to 2018," *Energy Rep.*, vol. 6, pp. 237–242, Dec. 2020, doi: 10.1016/j.egyr.2020.11.116.

[2] I. Hamdan, A. Alfouly, and M. A. Ismeil, "Hosting capacity enhancement for photovoltaic systems at various conditions based on Volt-Var control," in *Proc. 23rd Int. Middle East Power Syst. Conf. (MEPCON)*, Cairo, Dec. 2022, pp. 1–8, doi: 10.1109/MEPCON55441.2022.10021815.

[3] REN21. (2022). *Renewables 2022 Global Status*. [Online]. Available: https://www.ren21.net/gsr-2022/

[4] D. Chathurangi, U. Jayatunga, S. Perera, A. P. Agalgaonkar, and T. Siyambalapitiya, "Comparative evaluation of solar PV hosting capacity enhancement using Volt-VAr and Volt-Watt control strategies," *Renew. Energy*, vol. 177, pp. 1063–1075, Nov. 2021, doi: 10.1016/j.renene.2021.06.037.

[5] S. M. Ismael, S. H. E. A. Aleem, A. Y. Abdelaziz, and A. F. Zobaa, "State-of-the-art of hosting capacity in modern power systems with distributed generation," *Renew. Energy*, vol. 130, pp. 1002–1020, Jan. 2019, doi: 10.1016/j.renene.2018.07.008.

[6] R. Xavier, B. Bekker, and M. J. Chihota, "Smart inverters in LV networks: A review of international codes and standards, and opportunities for South Africa," in *Proc. Southern Afr. Univ. Power Eng. Conf./Robot. Mechatronics/Pattern Recognit. Assoc. South Afr. (SAUPEC/RobMech/PRASA)*, Jan. 2021, pp. 1–6, doi: 10.1109/SAUPEC/RobMech/PRASA52254.2021.9377224.

[7] T. Gush, C.-H. Kim, S. Admasie, J.-S. Kim, and J.-S. Song, "Optimal smart inverter control for PV and BESS to improve PV hosting capacity of distribution networks using slime mould algorithm," *IEEE Access*, vol. 9, pp. 52164–52176, 2021, doi: 10.1109/ACCESS.2021.3070155.

[8] S. Sakar, M. E. Balci, S. H. E. A. Aleem, and A. F. Zobaa, "Increasing PV hosting capacity in distorted distribution systems using passive harmonic filtering," *Electr. Power Syst. Res.*, vol. 148, pp. 74–86, Jul. 2017, doi: 10.1016/j.epsr.2017.03.020.

[9] E. Kazemi-Robati, M. S. Sepasian, H. Hafezi, and H. Arasteh, "PV-hosting-capacity enhancement and power-quality improvement through multiobjective reconfiguration of harmonic-polluted distribution systems," *Int. J. Electr. Power Energy Syst.*, vol. 140, Sep. 2022, Art. no. 107972, doi: 10.1016/j.ijepes.2022.107972.

[10] A. F. Zobaa, S. H. E. A. Aleem, S. M. Ismael, and P. F. Ribeiro, *Hosting Capacity for Smart Power Grids*. Berlin, Germany: Springer, 2020, doi: 10.1007/978-3-030-40029-3.

[11] M. Bajaj and A. K. Singh, "Hosting capacity enhancement of renewable-based distributed generation in harmonically polluted distribution systems using passive harmonic filtering," *Sustain. Energy Technol. Assessments*, vol. 44, Apr. 2021, Art. no. 101030, doi: 10.1016/j.seta.2021.101030.

[12] M. Bajaj and A. K. Singh, "Optimal design of passive power filter for enhancing the harmonic-constrained hosting capacity of renewable DG systems," *Comput. Electr. Eng.*, vol. 97, Jan. 2022, Art. no. 107646, doi: 10.1016/J.COMPELECENG.2021.107646.

[13] L. D. Campello, P. M. Duarte, P. F. Ribeiro, and T. E. de Oliveira, "Hosting capacity of a university electrical grid considering the inclusion of wind-turbines for different background distortions," in *Proc. 17th Int. Conf. Harmon. Quality Power (ICHQP)*, Oct. 2016, pp. 1026–1031, doi: 10.1109/ICHQP.2016.7783335.

[14] M. Bajaj, S. Aggarwal, and A. K. Singh, "Power quality concerns with integration of RESs into the smart power grid and associated mitigation techniques," in *Proc. IEEE 9th Power India Int. Conf. (PIICON)*, Feb. 2020, pp. 1–6, doi: 10.1109/PIICON49524.2020.9113008.

[15] J. Ballingston, *IEEE Recommended Practice and Requirements for Harmonic Control in Electric Power Systems*, IEEE Standard 519-2014, 2014, p. 101.

[16] *IEEE Standard for Interconnection and Interoperability of Distributed Energy Resources With Associated Electric Power Systems Interfaces*, IEEE Standard 1547, 2018, pp. 1–138.

[17] M. Bajaj and A. K. Singh, "A global power quality index for assessment in distributed energy systems connected to a harmonically polluted network," *Energy Sources A, Recovery, Utilization, Environ. Effects*, pp. 1–27, Jun. 2021, doi: 10.1080/15567036.2021.1929577.

[18] M. Bajaj and A. K. Singh, "Grid integrated renewable DG systems: A review of power quality challenges and state-of-the-art mitigation techniques," *Int. J. Energy Res.*, vol. 44, no. 1, pp. 26–69, Jan. 2020, doi: 10.1002/er.4847.

[19] M. Bajaj and A. K. Singh, "An analytic hierarchy process-based novel approach for benchmarking the power quality performance of grid-integrated renewable energy systems," *Electr. Eng.*, vol. 102, no. 3, pp. 1153–1173, Sep. 2020, doi: 10.1007/s00202-020-00938-3.

[20] M. Bajaj, A. Flah, M. Alowaidi, N. K. Sharma, S. Mishra, and S. K. Sharma, "A Lyapunov-function based controller for 3-phase shunt active power filter and performance assessment considering different system scenarios," *IEEE Access*, vol. 9, pp. 66079–66102, 2021, doi: 10.1109/ACCESS.2021.3075274.

[21] M. Bajaj, A. K. Singh, M. Alowaidi, N. K. Sharma, S. K. Sharma, and S. Mishra, "Power quality assessment of distorted distribution networks incorporating renewable distributed generation systems based on the analytic hierarchy process," *IEEE Access*, vol. 8, pp. 145713–145737, 2020, doi: 10.1109/ACCESS.2020.3014288.

[22] A. Alfouly, I. Hamdan, and M. Ismeil, "Voltage profile of hosting capacity enhancement based on smart inverter reactive power control for PV grid connected system," *SVU-Int. J. Eng. Sci. Appl.*, vol. 4, no. 2, pp. 234–242, Dec. 2023, doi: 10.21608/SVUSRC.2023.194712.1106.

[23] K. Luo and W. Shi, "Comparison of voltage control by inverters for improving the PV penetration in low voltage networks," *IEEE Access*, vol. 8, pp. 161488–161497, 2020, doi: 10.1109/ACCESS.2020.3021079.

[24] Y. Naderi, S. H. Hosseini, S. G. Zadeh, B. Mohammadi-Ivatloo, J. C. Vasquez, and J. M. Guerrero, "An overview of power quality enhancement techniques applied to distributed generation in electrical distribution networks," *Renew. Sustain. Energy Rev.*, vol. 93, pp. 201–214, Oct. 2018, doi: 10.1016/j.rser.2018.05.013.

[25] P. K. Madaria, M. Bajaj, S. Aggarwal, and A. K. Singh, "A grid-connected solar PV module with autonomous power management," in *Proc. IEEE 9th Power India Int. Conf. (PIICON)*, Feb. 2020, pp. 1–6, doi: 10.1109/PIICON49524.2020.9113065.

[26] F. AlAlamat, "Increasing the hosting capacity of radial distribution grids in Jordan," B.Sc. thesis, Uppsala Univ., Uppsala, Sweden, 2015.

[27] X. Sun, J. Qiu, and J. Zhao, "Optimal local Volt/Var control for photovoltaic inverters in active distribution networks," *IEEE Trans. Power Syst.*, vol. 36, no. 6, pp. 5756–5766, Nov. 2021, doi: 10.1109/TPWRS.2021.3080039.

[28] A. M. Howlader, S. Sadoyama, L. R. Roose, and Y. Chen, "Active power control to mitigate voltage and frequency deviations for the smart grid using smart PV inverters," *Appl. Energy*, vol. 258, Jan. 2020, Art. no. 114000, doi: 10.1016/j.apenergy.2019.114000.

[29] S. H. E. A. Aleem, M. E. Balci, and S. Sakar, "Effective utilization of cables and transformers using passive filters for non-linear loads," *Int. J. Electr. Power Energy Syst.*, vol. 71, pp. 344–350, Oct. 2015, doi: 10.1016/j.ijepes.2015.02.036.

[30] A. F. Zobaa, "Optimal multiobjective design of hybrid active power filters considering a distorted environment," *IEEE Trans. Ind. Electron.*, vol. 61, no. 1, pp. 107–114, Jan. 2014, doi: 10.1109/TIE.2013.2244539.

[31] S.-J. Jeon, "Non-sinusoidal power theory in a power system having transmission lines with frequency-dependent resistances," *IET Gener. Transmiss. Distrib.*, vol. 1, no. 2, pp. 331–339, Mar. 2007, doi: 10.1049/iet-gtd:20050446.

[32] M. Gunawardana, A. Ng, and B. Kordi, "Time-domain coupling model for nonparallel frequency-dependent overhead multiconductor transmission lines above lossy ground," *IEEE Trans. Power Del.*, vol. 37, no. 4, pp. 2997–3005, Aug. 2022, doi: 10.1109/TPWRD.2021.3121194.

[33] R. Sinvula, K. M. Abo-Al-Ez, and M. T. Kahn, "Harmonic source detection methods: A systematic literature review," *IEEE Access*, vol. 7, pp. 74283–74299, 2019, doi: 10.1109/ACCESS.2019.2921149.

[34] M. Kumawat, N. Gupta, N. Jain, and R. C. Bansal, "Optimal planning of distributed energy resources in harmonics polluted distribution system," *Swarm Evol. Comput.*, vol. 39, pp. 99–113, Apr. 2018, doi: 10.1016/j.swevo.2017.09.005.

[35] M. A. Ismeil, I. Hamdan, and A. Alfouly, "Impact of active power control for hosting capacity grid-connected PV systems," *J. Electr. Power Syst. Eng.*, vol. 9, no. 2, pp. 32–42, 2023. [Online]. Available: https://matjournals.co.in/index.php/JEPSE/article/view/2716/3537

[36] M. Bajaj, "Design and simulation of hybrid DG system fed single-phase dynamic voltage restorer for smart grid application," *Smart Sci.*, vol. 8, no. 1, pp. 24–38, Jan. 2020, doi: 10.1080/23080477.2020.1748928.

[37] M. Bajaj and A. K. Singh, "Designing of a solar energy based single phase dynamic voltage restorer using fuzzy logic controlled novel boost inverter," in *Proc. IEEE 9th Power India Int. Conf. (PIICON)*, Feb. 2020, pp. 1–6, doi: 10.1109/PIICON49524.2020.9112965.

[38] *IEEE Recommended Practice and Requirements for Harmonic Control in Electric Power Systems*, IEEE Standard 519-2014, IEEE Power and Energy Society (Transmission and Distribution Committee), 2014.
[39] A. Hiranandani, "Calculation of cable ampacities including the effects of harmonics," *IEEE Ind. Appl. Mag.*, vol. 4, no. 2, pp. 42–51, 1998, doi: 10.1109/2943.655660.

MOHAMED A. ISMEIL (Member, IEEE) was born in Qena, Egypt, in October 1977. He received the B.Sc. and M.Sc. degrees in electrical engineering from South Valley University, in 2002 and 2008, respectively, and the Ph.D. degree from the Channel System Program, Aswan University, in April 2014. Since November 2002, he has been an Associate Professor with the College of Engineering, King Khalid University, Saudi Arabia. From October 2010 to January 2013, he was a Ph.D. Student with the Department of Electrical Drive Systems and Power Electronics, Technical University of Munich, Germany. From April 2014 to September 2018, he was an Assistant Professor with the Aswan Faculty of Engineering, Aswan University. Since October 2018, he has been an Associate Professor with the Qena Faculty of Engineering, South Valley University. From March 2020 to November 2002, he was the Head of the Electrical Department, Qena Faculty of Engineering. He has published more than 45 papers in international conferences and journals. His current research interests focus on power electronics applications in wind energy conversion systems, PV interface with the utility, smart grid technologies, and digital control applications (PIC, FPGA, and DSP). His main interest is power inverter design for renewable applications.

AHMED ALFOULY was born in Qena, Egypt, in July 1996. He received the B.Sc. degree in electrical engineering from South Valley University, in 2019. He is currently a Teaching Assistant with the Faculty of Engineering, South Valley University. His research interests include the integration of renewable energy sources, PV/wind hybrid power systems, power electronics, and control of the smart grid and microgrid systems.

HANY S. HUSSEIN (Senior Member, IEEE) received the B.Sc. degree in electrical engineering and the M.Sc. degree in communication and electronics from South Valley University, Egypt, in 2004 and 2009, respectively, and the Ph.D. degree in communication and electronics engineering from the Egypt–Japan University of Science and Technology (E-JUST), in 2013. In 2012, he was a Special Researcher Student with Kyushu University, Japan. He has been an Associate Professor with the Faculty of Engineering, Aswan University, since 2019. He is currently an Assistant Professor with the College of Engineering, King Khalid University, Saudi Arabia. His research interests include digital signal processing for communications, multimedia, image, and video coding, low-power wireless communications, one-bit ADC multiple-input multiple-output, underwater communication, index, and spatial modulation, Li-Fi technology, and visible light communication. He is a technical committee member of many international conferences and a reviewer of many international conferences, journals, and transactions. He was the General Co-Chair of the IEEE ITCE, in 2018.

I. HAMDAN was born in Qena, Egypt, in 1985. He received the B.Sc. and M.Sc. degrees in industrial electronics and control engineering from the Faculty of Electronic Engineering, Menoufia University, Egypt, in 2008 and 2015, respectively, and the Ph.D. degree from the Department of Electrical Engineering, Faculty of Engineering, South Valley University, Egypt, in 2019. He is currently an Assistant Professor with the Department of Electrical Engineering, Faculty of Engineering, South Valley University. His current research interests include control engineering, artificial intelligence, large-scale systems, and renewable energy systems.